Jurnal Mekanikal
Disember 2001, Bil. 12, 47- 58

ANALYSIS OF WARM POWDER COMPACTION PROCESS USING FINITE ELEMENT MODEL

A. K. Ariffin
Md. Mujibur Rahman

Dept. of Mechanical and Materials Engineering
Universiti Kebangsaan Malaysia
43600 Bangi, Selangor Darul Ehsan
MALAYSIA

ABSTRACT

This paper presents the development of the finite element model for the simulation of a full cycle of warm powder compaction process. In the modelling of compaction phase, the behaviour of powder is assumed to be rate independent thermo-elastoplastic material and the process has been described by a large displacement based finite element formulation. Two constitutive relations namely Mohr-Coulomb yield criterion and Elliptical Cap yield criterion have been used to describe the mechanical behaviour of the powder during the compaction. The staggered-incremental-iterative solution strategy has been established to solve the non-linear systems of equations. The numerical results are validated by experiments, which show a good agreement between the simulation and experiment data.

Keywords: *Warm compaction, finite element method, staggered-incremental-iterative.*

1.0 INTRODUCTION

The production of solid component from metal powders by compaction and sintering is known as powder metallurgy (P/M). In order to expand the market and give lowest total cost, efforts to improve P/M technology have focused on ways to enhance the mechanical properties and tolerances of the finished parts. A major advance in P/M technology has been the warm compaction process, which produces changes in the pore morphology of sintered parts compared to that obtained by cold compaction. The result is that higher density levels are obtained and at the same time warm compaction products have more even density distribution. These will lead to higher strength and better dimensional tolerances.

The warm compaction process can utilise traditional powder metallurgy compaction equipment and is applicable to most powder/material systems but requires that both the powder and the die assembly are heated up to a temperature in the range of 100-150°C. The temperature range 100-150°C roughly delimits the working temperature because at the temperature above 150°C, lubricants begin to break down and at the higher temperatures iron powders oxidise more rapidly. However, at temperatures below about 100°C, sufficient compaction effect cannot be achieved [1].

In order to heating up the powder, three different technologies exist today, i.e., slot heater, el-temp and Abbot. Slot heater uses a conventional heat exchanger with oil-heated elements where the powder is free flowing to the filling shoe and the die. El-temp utilises a heated screw feeder, which together with heating the powder, transports it to the filling show. Lastly, Abbot heater transfers heat to the powder with a fluidised bed. In warm compaction process, the die assembly must also be heated up together with the powder mass.

There is a significant influence of temperature on deformation behaviour. Deformation of metals can be looked upon as thermally activated process where both the elastic and plastic deformations are affected [2]. The microscopical mechanisms that explain this behaviour are complex. Higher temperature gives lower deformation resistance, which is quantified by yield strength.

An analysis of the powder compaction process is important since this gives an insight into the compaction process and reduces the risk of designing and manufacturing inappropriate components and tools. Hence, the objective of this study is to develop a finite element model to represent the complete cycle warm powder compaction process. This includes experimental investigation to establish material parameters and data to validate the model.

In powder compaction modelling, the powder can be represented by a micromechanical scale [2] or by the basis of a continuum [3,4]. The former approach focuses on powder particles, which practically have a variety of shape, size, hardness and arrangement within the compact. This kind of approach may be useful in investigating the effect of particle characteristics during the compaction and the compact [5]. The later approach considered the powder as a continuum rather than an assemblage of individual particles. This approach can provide information on the global behaviour of the powder mass such as the powder movement, density distribution, stress states and the shape of the compact during and after the compaction [6].

Using the continuum framework, the formulation can be done either based on load control or displacement control. The former approach is suitable for non-linear analysis such as reinforced concrete structures [7]. Some of the problems associated with load control approach include the inability to capture responses on the falling branch of the load-displacement relationship. However, the later approach is more suitable to model the compaction behaviour of powder materials since at low density levels, a large deformation can be resulted by a small amount of load.

In the case of powder forming, the simulation must capture the large displacements, which occur. Several researchers have proposed and utilised finite element schemes for problems of large displacements, and these include diverse formulations of both the Eulerian and Lagrangian type. In Eulerian procedure, the physical quantities are expressed as a function of time and position vector in the geometric space. Using this approach, McMeeking and Rice [8] presented a

finite element formulation for the problem of large elastic-plastic flow. The method is based on Hill's variational principle for incremental deformations and is ideally suited to isotropically Prandtl-Reuss materials and high-speed deformation.

In Lagrangian strategy, the element geometry changes are determined by the deformation of the material. Brekelmans et al. [9] modelled the complex shaped die compaction process using the total Lagrangian strategy. In this procedure, the original element mesh was sufficiently accurate for any changes in physical quantity and material properties are captured accurately. However, instability may occur in the case of highly non-linear calculation where more than one material properties are considered in one element. In order to overcome the problems associated with the total Lagrangian strategy, an updated Lagrangian strategy may be applied where the coordinates of the finite element mesh have to be referred to the previous calculation steps. Park et al. [10] developed a finite element model for the cold compaction of metal powders in which the updated Lagrangian strategy has been utilized. However, difficulties still arise in analyses, which involve large displacements because the element shapes can still become highly distorted leading to an unreliable solution due to mesh degeneration.

The present paper deals with simulation and experimental work for a complete cycle in the generation of a green compact. The rate independent elastoplastic with a displacement based finite element formulation was applied in the simulation work. The Mohr-Coulomb and Elliptical Cap yield models were used to represent the behaviour of powder under loading. The material and boundary conditions were established from warm compaction experiment.

2.0 GOVERNING EQUATIONS

The warm compaction process has been modelled using a thermo-elastoplastic constitutive law where the axisymmetric simulations are used to represent the process. In the mathematical model, the constitutive laws of powder are described first continued by the heat conduction model.

2.1 Constitutive Model of Powder

The behaviour of stress and strain are characterised by a non-linear relationship started from the beginning of the compaction stage. The momentum balance or Cauchy's first law of motion can be written as

$$\rho \mathbf{b} + \mathbf{div}\,\sigma = 0 \tag{1}$$

where ρ is the mass density, $\mathbf{b}$ is the body force and σ is the Cauchy's stress tensor.

The total strain increment is assumed to be the sum of elastic strain $d\varepsilon^e$ increment, plastic strain increment $d\varepsilon^p$ and thermal strain increment $d\varepsilon^{th}$ as

$$d\varepsilon_{ij} = d\varepsilon_{ij}^{e} + d\varepsilon_{ij}^{p} + d\varepsilon_{ij}^{th} \tag{2}$$

Incorporating the elasticity matrix $\mathbf{D}_e$ and using the hardening rule and associated flow rule, the elastic and plastic strain increment can be written as

$$d\varepsilon_e = \mathbf{D}_e^{-1} d\sigma \text{ and } d\varepsilon_p = d\gamma \frac{\partial Q}{\partial \sigma} \tag{3}$$

where γ is the plastic multiplier and $\partial Q/\partial\sigma$ is the plastic flow potential. The thermal strain increment can be written as

$$d\varepsilon_{th} = \frac{1}{3} m\alpha dT \tag{4}$$

where α is the thermal expansion coefficient. For an isotropic material, the yield criterion may be formulated as

$$F = f(\sigma, h, T) \tag{5}$$

In this study, Mohr-Coulomb yield model and Elliptical Cap yield model are considered. The Mohr-Coulomb yield model can be expressed mathematically as

$$F = J_1 \sin\varphi + \sqrt{J_{2D}}\cos\theta - \sqrt{\frac{J_{2D}}{3}}\sin\theta\sin\varphi - c\cos\varphi = 0 \tag{6}$$

where J_1 and J_{2D} are the first and second invariant deviatoric stress. The Elliptical Cap yield model can be expressed mathematically as

$$F = 3J_{2D} + M^2 J_1 (J_1 + 2\sigma_c) = 0 \tag{7}$$

From equations (4) and (5), the total strain increment can be expressed as

$$d\varepsilon = \mathbf{D}_e^{-1} d\sigma + d\gamma \frac{\partial Q}{\partial \sigma} + \frac{1}{3} m\alpha dT \tag{8}$$

After partially differentiate the yield criterion in equation (5), and using equation (8), the thermo-elastoplastic constitutive relationship can be written as

$$d\sigma = \mathbf{D}_{ep}\left[d\varepsilon - \left(m\frac{\beta_s}{3} - \frac{\dfrac{\partial Q}{\partial \sigma}\left(\dfrac{\partial F}{\partial h}\dfrac{\partial h}{\partial T} + \dfrac{\partial F}{\partial T} \right)}{\dfrac{\partial F}{\partial h}\left\{ \dfrac{\partial h}{\partial \varepsilon^p} \right\}^{\mathrm{T}} \dfrac{\partial Q}{\partial \sigma}} \right) dT \right] \tag{9}$$

where $\mathbf{D}_{ep}$ is the elastoplastic tangent modulus.

2.2 Thermal Analysis

During the warm compaction process, the powder mass and the die are heated up to an elevated temperature prior to the compaction. The elevated temperature is also due to the plastic deformation and friction between the compacted powder and tooling. The coupling between mechanical and thermal phenomena for axisymmetric case can be written as

$$\frac{1}{r}\frac{\partial}{\partial r}\left(rk\frac{\partial T}{\partial r} \right) + \frac{\partial}{\partial z}\left(k\frac{\partial T}{\partial z} \right) + Q_h = \rho C_h \frac{\partial T(r,t)}{\partial t} \tag{10}$$

where r is radius, Q_h is heat generation and C_h is specific heat. The thermal conductivity k in equation (10) depends on the relative density of the compact because heat transfer through a loosely packed powder is less rapid than a consolidated body.

3 FINITE ELEMENT FORMULATION

The finite element technique is used to formulate a computational framework for integration of the mathematical models defined in the previous section.

3.1 Mechanical Problem

For the purpose of finite element discretization, six noded isoparametric triangular elements are considered. Displacement based thermo-elastoplastic model has been formulated by using the principle of virtual work and considering the non-linear material behaviour as

$$\int_{\Omega} \boldsymbol{\sigma}\delta\boldsymbol{\varepsilon} d\Omega - \int_{\Omega} \rho \mathbf{b}\delta\mathbf{a} d\Omega - \int_{\Gamma} \mathbf{F}\delta\mathbf{a} d\Gamma = \mathbf{f}^e \tag{11}$$

where Ω is domain area and Γ is surface length. The global displacement equation can be written as

$$[\mathbf{K}]\{\Delta\mathbf{a}\}+\{\mathbf{F}\}=0 \tag{12}$$

where $[\mathbf{K}]$ represents the stiffness matrix, $\{\Delta\mathbf{a}\}$ represents the unknown displacement and $\{\mathbf{F}\}$ represents the force vector. The tangential stiffness matrix is given by

$$[\mathbf{K}]=\int_{\Omega}\mathbf{B}^{\mathrm{T}}\frac{\partial\sigma}{\partial\varepsilon}\mathbf{B} \tag{13}$$

where **B** is the strain displacement matrix.

3.2 Thermal Problem

The finite element discretization procedure used to solve mechanical problem is also used to solve thermal problem. The Galerkin weighted residual method is employed for the development of the finite element solution scheme. The temperature distribution within each element can be approximated by

$$\theta(\xi,\eta)=\sum_{j=1}^{n}N_j(\xi,\eta)T_j \tag{14}$$

The rate of change of temperature with respect to time is

$$\dot{T}_{n+1}=\frac{T_{n+1}-T_n}{\Delta t} \tag{15}$$

where T_n is the known temperature at time t_n and T_{n+1} is the unknown temperature at time t_{n+1}. The final equation including stiffness matrix can be expressed as

$$(\mathbf{C}_{n+1}+\mathbf{K}_{n+1})T_{n+1}=\mathbf{F}_{n+1}+\mathbf{C}_{n+1}T_n \tag{16}$$

The matrices **C**, **K** and **F** include the non-linear thermal properties where they are evaluated at time t_{n+1}. In linear discretization form, the equation (16) becomes

$$\overline{\mathbf{K}}_{n+1}T_{n+1}=\overline{\mathbf{F}}_{n+1} \tag{17}$$

The temperature calculation in equation (17) is treated in a consecutive manner where the mechanical equilibrium system is first fulfilled so that the matrix **F** is found at time t_n. The initial temperature is given at the first time step as T_0.

3.3 Solution Procedure

A staggered-incremental-iterative solution procedure is applied to achieve a suitable solution of the mechanical as well as thermal equations because they are highly non-linear due to the consideration of thermo-elastoplastic material constitutive law. The coupled thermomechanical computational flowchart using staggered-incremental-iterative solution procedure can be seen in Figure 1.

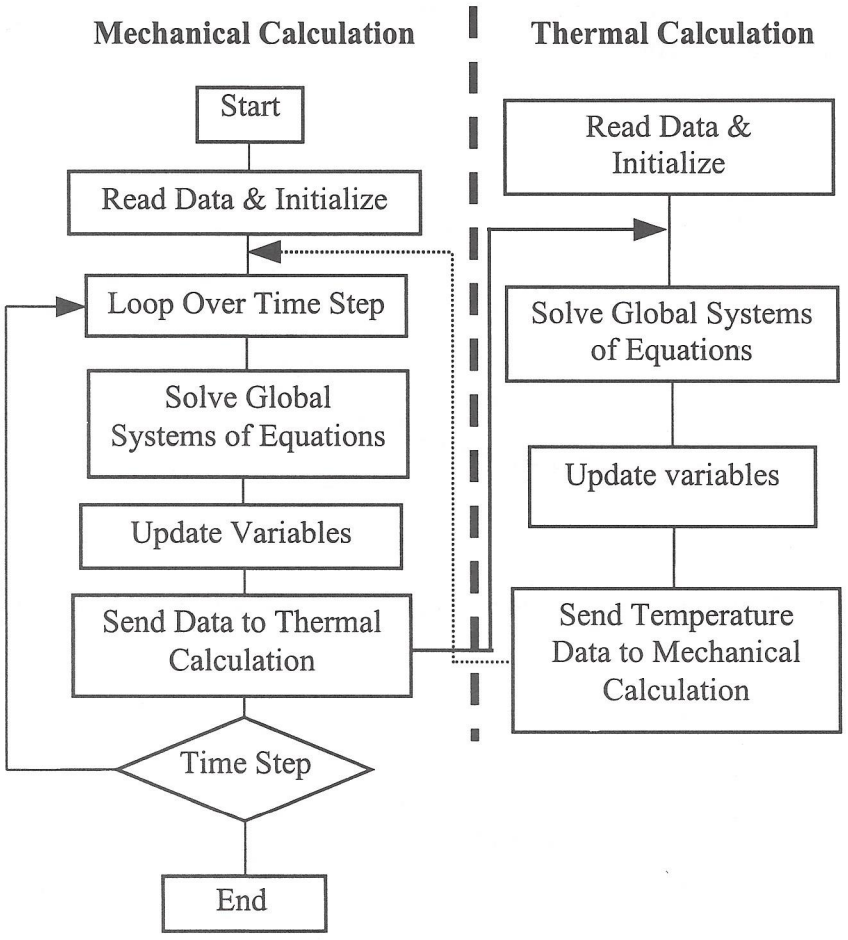

Figure 1 Summary of Complete Computational Procedure

4.0 RESULTS AND DISCUSSION

The numerical simulation of warm compaction process has been modelled to generate a green compact of simple plain bush component. Since a displacement based formulation is adopted, the implementation of loading in the finite element code is achieved by the use of prescribed nodal displacements. The direction of

this displacement is always in a vertical plane, which represents the axial punch load.

Figure 2 illustrates the axial stress with respect to compaction strain for the compaction at room temperature and elevated temperature. The compaction at elevated temperature produces a lower stress compared to the compaction at room temperature. This is caused the shrinkage of yield surface due to heating up the powder mass prior to compaction. The physical meaning of this phenomenon is that in warm compaction process, a considerable lower force is required to obtain a specific displacement.

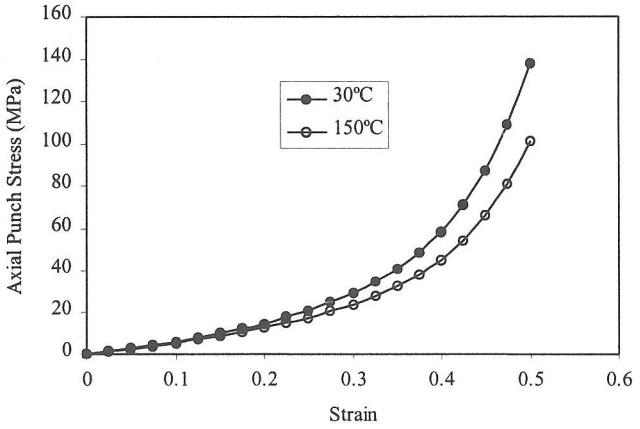

Figure 2 Stress Development with Compaction Strain at different temperature

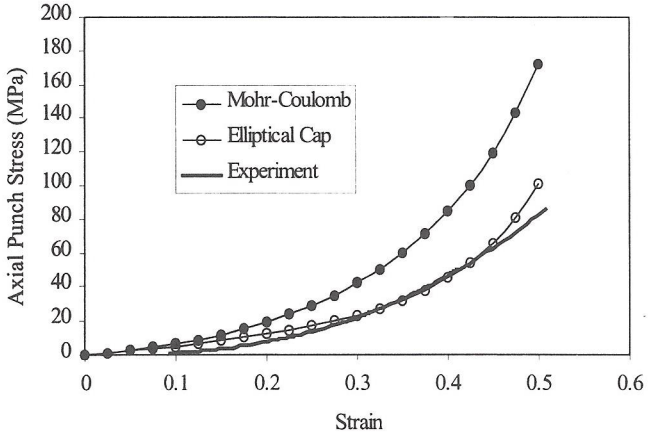

Figure 3 Stress Development with Compaction Strain

Figure 3 shows the force-balance results presented as stress-strain curves for the compaction phase simulation where the two yield models are compared with the experimental data. In general, these two models show similar trend with respect to stress development against strain. However, the stress level predicted is different for each model. The Mohr-Coulomb yield model produces the higher stress compared to Elliptical Cap model. In Elliptical Cap yield model, there is a critical state line which limits the elastic and inelastic deformations. No stress state should be above this critical state line. Any stress state inside the yield surface in Mohr-Coulomb yield model may be above the critical state line in Elliptical Cap yield model. Hence the stress predicted by Elliptical Cap yield model is lower than that of Mohr-Coulomb yield model. The close agreement with experimental data are achieved by the Elliptical Cap yield model.

A considerable elastic recovery or spring back has been occurred during the relaxation phase. Figure 4 shows the comparison of the predicted between the cold and warm results for the relaxation phase. The amount of spring back is higher in warm compaction compared to the cold compaction. Higher maximum spring back was also found in the experiment.

Figure 5 illustrates the density variations from the top to the bottom of the compact. Warm compaction process produces the more uniform density distribution compared to cold compaction process. This is highly desired in powder compaction industry to avoid the initiation of internal cracks or shape distortion of the compact after sintering due to non-uniform density distribution within the green compact.

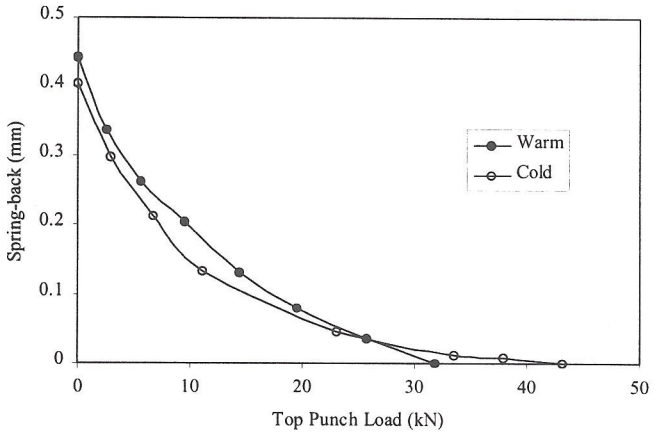

Figure 4 Cold and Warm Results on Spring-back during Unloading of Top Punch

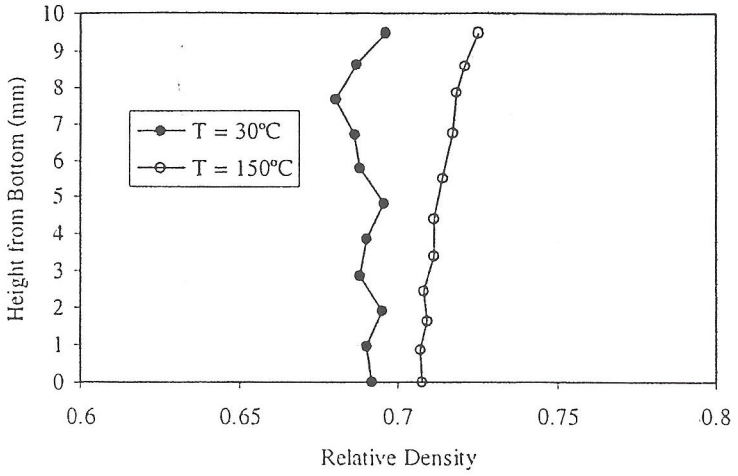

Figure 5 Relative Density with Compact Height for Cold and Warm Compaction Model

Figure 6 shows the predicted ejection force for the compaction at different temperature. A higher force is required to initiate the ejection process for the compaction at elevated temperature. This is due to the sticking phenomenon of metal powder compact with the die at elevated temperature. Just after the compaction phase, the compact may expand which gives a higher radial force. Therefore, in order to overcome this higher radial force, a relatively higher force is required to eject the powder compact from the die cavity

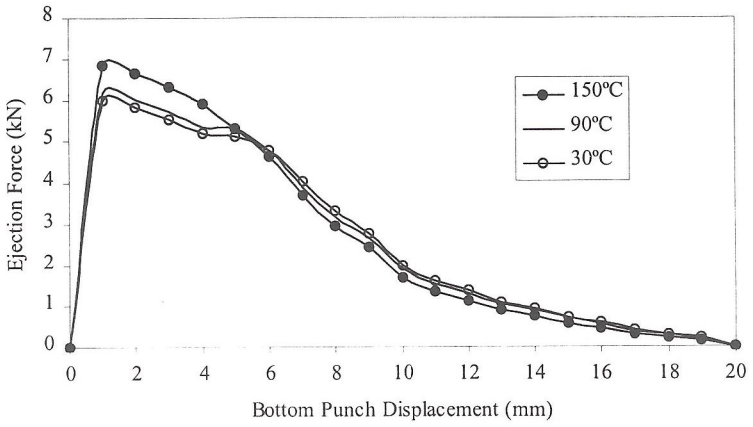

Figure 6 Predicted Results for Ejection and Emergence at Different Temperature

5.0 CONCLUSION

A coupled thermal-mechanical model of warm powder compaction process was developed in the generation of green compact. Two yield models were used to represent the deformation behaviour of metal powder mass during the deformation process. The results are compared with the warm compaction experimental data. An Elliptical Cap yield model is suitable to represent the behaviour of warm metal powder mass during the compaction phase. The warm compaction model produces the more uniform density distribution. A considerable spring-back occurred during the relaxation phase. In warm compaction process, higher load is required to initiate the ejection process.

ACKNOWLEDGEMENT

This research is supported by the Ministry of Science Technology and Environment Malaysia through the research project IRPA 03-02-02-0048.

REFERENCES

1. Höganas , A. B., 1998, Höganas hand book for warm compaction.
2. Jogata, A., Dawson, P. R. & Jenkins, J. T., 1988, *An Anisotropic Continuum Model for the Sintering and Compaction of Powder Packing*, Mechanics of Materials, 7, pp. 255-269.
3. Brown, S. B. and Weber, G. G. A., 1988, *A Constitutive Model for the Compaction of Metal Powders*, Modern Development in Powder Metallurgy, vol.18-21, pp.465-476.
4. Oldenburg, M. and Haggbald, H. A., 1994, *Material Parameter Fitting in an Integrated Environment for Analysis of Iron Powder Pressing*, Powder Metallurgy World Congress, vol.1, June, Paris, pp.693-696.
5. Hisatsune, T., Tabata, T. & Masaki, S., 1991, *A Yield Criterion of Porous Material With Anisotropy Caused By Geometry or Distribution of Pores*, J. Eng. Mat. Tech., Trans. ASME, Oct., vol.113, pp.425-429.
6. Cytermann, R. & Geva, R., 1987, *Powder Metallurgy*, Development of New Model for Compaction of Powders, vol.30, no.4, pp.256-260.
7. May, I. M., Naji, J. H. and Ganaba, T. H. , 1988, *Displacement Control for the non-linear analysis of reinforced concrete structures*. Engineering Computations, 5, 266.
8. McMeeking, R. M. and Rice, J. R. , 1975, *Finite Element formulation for problems of large elastic-plastic deformation*. Int. J. of Solid Structures, 11, 601.

9. Brekelmans, W. A. M., Janssen, J. D., Van de Ven, A. A. F. & de With, G., 1991, *An Eulerian Approach for Die Compaction Processes*, Int. J. Num. Meth. Eng., vol.31, pp.509-524.
10. Park, S., Han, H. N., Oh, H. K.and Lee, N. D., 1999. *Model for Compaction of Metal Powders*, International Journal of Mechanical Sciences. 41: 121-141.